Computer Communications 136 (2019) 1–9

Contents lists available at ScienceDirect

Computer Communications

journal homepage: www.elsevier.com/locate/comcom

Cost-effective fiber fault monitoring using MLMW-OOCs in high-capacity PONs considering user geographical distribution[☆]

Min Zhu [a,*,1], Shengyu Zhang [b], Guixin Li [b], Jiao Zhang [b]

[a] National Mobile Communications Research Laboratory, Southeast University, Nanjing, 210096, China
[b] School of Electronic Science and Engineering, Southeast University, Nanjing, 210096, China

ARTICLE INFO

Keywords:
Passive optical networks (PONs)
Fiber fault monitoring
Signal-to-interference-ratio (SIR)
Multiple length multiple wavelength optical orthogonal codes (MLMW-OOCs)

ABSTRACT

Cost-effective monitoring of in-service passive optical network (PON) link is becoming increasing important for network operators. Recently, optical coding schemes based on 1D-PCs or 2D-OOCs for PON link monitoring have been proposed. Note that these codes are equal-length, and are assigned randomly to each user in PON. Hence there may be severe interferences, especially in the case that user separation length is close to each other. Moreover, when the number of users (i.e., user network size) is larger, the code length becomes abnormally large, which makes these existing schemes infeasible in practice. In this paper, we propose a novel codeword assignment scheme based on multiple-length multiple-wavelength optical orthogonal codes (MLMW-OOCs) for realistic PON link fault monitoring. In the novel codeword assignment, the information on user geographical distribution is additionally considered to minimize the inter-user interferences. The mathematical expressions of system signal-to-interference-ratio (SIR) are analyzed with aid of a new parameter "interference ratio". The extensive simulation results show that the SIR of the MLMW-OOC-based scheme performs better than that of the 2D-OOCs scheme. Moreover, our proposed scheme can support the effective monitoring for high-capacity PONs with the shorter code length, the smaller correlation distance, and hence present the higher system SIR performances.

1. Introduction

PASSIVE optical networks (PONs) have been considered the best choice of the telecom operators in the first/last mile optical access network solutions, as its passive low-power components, cost effectiveness, service transparency, and higher security [1]. With the huge amount of Fiber to the Home/Building (FTTH/B) PONs being deployed massively, the large part of maintenance expense on monitoring fiber faults occurs within the first/last mile. Therefore, cost-effective, in-service, and practical optical layer performance monitoring mechanism is becoming more and more significant [2,3].

Optical Time Domain Reflectometry (OTDR) based monitoring techniques presents severe limitations when applied in point-to-multipoint (PTMP) PONs [4]. Hence, Optical Coding (OC) based technique has been proposed recently for the optical-layer monitoring of PON links [5–11]. The unique optical code is assigned randomly to each user in a PON, to monitor the individual distribution drop fiber (DDF) of the each optical network unit (ONU) user. The passive encoder placed at the edge of the DDF generates pseudo orthogonal codes to identify each user from the other.

A modified one dimensional optical periodic coding (1D-PC) scheme has been proposed and demonstrated experimentally by using fiber Bragg grating (FBG) encoders [6,7]. However, the 1D-PC monitoring scheme suffers from serious challenges in practical deployments. With the increasing number of users in a PON, the required encoder length of the 1D-PCs increases significantly. Not only does that increase greatly the fabrication cost of the optical encoder, but it may make the 1D-PCs based monitoring scheme infeasible (see more in our simulation part). In addition, the code length and correlation distance of the 1D-PCs also increases rapidly as the increase of network size. It results in poor signal-to-interference-ratio (SIR) of monitoring signals, due to the fact that the larger correlation distance increases the interference effects. It finally leads to the serious degradation of the monitoring system performance. Hence, two dimensional wavelength-time optical orthogonal codes (2D-OOCs) was proposed [8,9] for serving a high-capacity PON with more users, as well as improving SIR of the monitoring signals for accurate fault-identification.

However, when serving a high-capacity PON with the much more users (e.g., 256 user or above), those limitations of the 1D-PC schemes still exist in the 2D-OOC based monitoring system. It is because that

☆ The work was supported by the National Natural Science Foundation of China (NSFC) (61771134).
* Corresponding author.
E-mail address: minzhu@seu.edu.cn (M. Zhu).
1 Member, IEEE.

https://doi.org/10.1016/j.comcom.2019.01.005
Received 4 August 2018; Received in revised form 1 January 2019; Accepted 11 January 2019
Available online 16 January 2019
0140-3664/

both the 1D-PCs and the 2D-OOCs are single-length codes, and they have the identical code length. They do not take advantage of the multiple-length 2D codes to minimize the maximum code length. Moreover, these existing optical coding schemes assign optical codes to all PON users just in a random way, and *do not consider user geographical distribution*, i.e., the information on user separation lengths (the length of DDFs). For example, when some DDF lengths are close to each other, it is easier to generate severe interferences and hence the SIR of the monitoring system should be degraded correspondingly, vice versa. In the case, to improve the monitoring system SIR performance, it is much better to assign the shorter codewords to these users close to each other, which may reduce inter-user interferences. Meanwhile, the fabrication cost of optical encoders with the shorter code length is lower correspondingly.

Our preliminary work was published in the conference paper [12]. But some technical details (e.g., theoretical analysis, system performance optimization, etc.) are not given out due to the limited space of the conference paper. In this paper, we present in detail a novel codeword assignment scheme based on multiple-length multiple wavelength optical orthogonal codes (MLMW-OOCs) for the link monitoring in a high-capacity PON, with the additional consideration of the user geographical distribution. Note that the information of user geographical distribution (i.e., the length of DDFs) is known for access network operator via the auto-discovery mechanism in PON, where the round-trip time (RTT) is learned automatically for each newly-connected ONU [1]. The novel scheme actually can reduce the partial interferences by assigning the shorter codes to those users, which are close geographically to each other. It cannot only reduce inter-user interferences as much as possible to improve the SIR of the monitoring system, but also makes the lengths of required codewords much shorter to reduce the fabrication cost of encoders. The two nice features make the novel scheme more feasible and practical. For the novel scheme, we also analyze mathematically the monitoring system SIR performance. A new parameter ''interference ratio'' is defined to make the SIR mathematical expression more precise. In simulations, we first compared the performances of two coding schemes (i.e., MLMW-OOC and 2D-OOC) in terms of the code length and the correlation distance under the different network sizes. The simulation results also show that our proposed codeword assignment scheme based on MLMW-OOCs performs much better than the random assignment scheme based on 2D-OOCs. Therefore, compared with the random scheme, for monitoring a certain capacity (i.e., network size) of PONs, our scheme is characterized by the shorter code length, the smaller correlation distance, and hence the higher SIR performances. In other words, given a required code length or a required SIR value, more PON customers can be served for DDF link monitoring, catering to a high-capacity PON.

The rest of this paper is organized as follows: In Section 2, the related works on PON link monitoring are introduced. In Section 3, after introducing some preliminary information about the MLMW-OOC construction method, we present the operation principle of the MLMW-OOC-based fiber fault monitoring system in a high-capacity PON. In Section 4, we then propose a codeword assignment scheme with the double-length MLMW-OOCs to minimize both the length of the required codes and the inter-user interferences. Meanwhile, we give out a more precise SIR mathematical expression. In Section 5, we compare and analyze the system performances of the different coding schemes. Finally, Section 4 concludes the paper.

2. Related Works on PON Link Monitoring

ITU-T G.984.2 and G.984.3 are two standards developed for GPON maintenance, which describe some physical layer measurements based on monitoring the active components (i.e., optical line terminal (OLT) and ONU. For instance, in GPON, when ONU detects loss of signal (LOS) or frame loss (LOF), it goes to POPUP state and stops sending upstream frames. In IEEE 802.3ah for standard EPON, during normal operation, ONU REPORTs reset OLT's watchdog timer. If the OLT's watchdog timer for the ONU times out, the ONU is de-registered. However, these standardized mechanisms using active component measurements and higher layer protocols to monitor the physical layer of PONs is inefficient and expensive for the network operator. Some major shortages are highlighted in [4], such as (i) a special numerical algorithm and additional processor capacity at both the OLT and ONUs are required, which increases the complexity, cost and repairing time; (ii) no preventive fault detection leads to error rate degradation and data loss; (iii) In the switching OFF scenarios, the monitoring information from these ONUs will be lost, thus the OLT confused about the real status of the branched fiber. Therefore, it is recommended that fault detection takes place at the layer closest to the failure, thus reducing the cross-layer signaling required for fault notification [13]. The above-mentioned works focus on the electrical-layer monitoring of PON links.

For the optical-layer monitoring of PON links, there are two main technical branches. First, conventional OTDR based monitoring techniques provide an efficient way to detect link-fault location away from the central office (CO) on point-to-point (PTP) optical fibers. However, they are ineffective on PTMP multi-branches PONs, because of the high optical attenuation and a composite trace which is difficult to be distinguished especially for increasing network size [1,4]. To solve this issue, a variety of modified OTDRs have been proposed to differentiate individual DDFs. These techniques include embedded OTDR, tunable OTDR, Brillouin OTDR, etc. [14–20]. Though the above methods partially overcome the limitations of conventional OTDR, they are still difficult to design and maintain after deployment for a high-capacity PON.

As an alternative solution, H. Fathallah, M.M. Rad et al. proposed OC-based monitoring technique, with which passive encoders are placed at the edge of the DDFs that generate pseudo orthogonal codes to identify each subscriber from the other [5–10]. Therefore, there is no need to use OTDR at the CO to detect if there is a fault in any DDF. Instead, the decoding system is placed at the CO to decode the codes coming from the different branch encoders. Thus the CO monitoring system can evaluate the status of all DDFs. This centralized monitoring technique significantly increases the scalability and reduces the system complexity. In [6,7], 1D-PC scheme was proposed and demonstrated experimentally by using multi-FBG (MFBG) encoders. But the 1D-PC scheme has some limitations as above stated. To enlarge code cardinality (which increases the number of PON users served correspondingly) as well as reduce the effect of interference on the received coding signal of the target user in a high-capacity PON, the optical coding scheme based on the 2D-OOCs was also proposed [8,9]. The construction methods of the 2D-OOCs have been researched in [10]. These codes can support larger-scale networks with shorter code length, and obtain better SIR performances due to the smaller correlation distance, compared with the 1D-PCs. In [21], authors gave an analytical expression of the average number of false detections and evaluated the system performance in terms of false detections in a PON monitoring scheme. The authors in [22] combined the OTDR scheme and the optical coding scheme in a dual-fiber ring-topology PON, which can realize both precise location of faulty point and identification of failed fiber link. Also, the protection scheme can be carried out once a faulty point is detected, thus saving recovery time.

3. MLMW-OOC-based fiber fault monitoring

3.1. MLMW-OOC construction method and one-hit probability analysis

To make the paper self-contained, some preliminary information about the MLMW-OOC construction method and the one-hit probability analysis [23,24] are also included in this paper. The MLMW-OOCs are represented by a family of ($m \times F$, w, λ_a, λ_c, D), where m is the number of wavelengths, F is a set of code lengths, w is code weight, λ_a is a set of autocorrelation constraints, λ_c is a set of cross-correlation constraints, D is a set of codeword-cardinality distribution ratio [23,24].

Table 1
Mlmw-oocs Short Codeword 10100, 5 Wavelengths, Code Weight 2, Code Length 5.

Group 0	Group 1	Group 2	Group 3	Group 4
$\lambda_0 0 \lambda_0 00$	$\lambda_0 0 \lambda_1 00$	$\lambda_0 0 \lambda_2 00$	$\lambda_0 0 \lambda_3 00$	$\lambda_0 0 \lambda_4 00$
$\lambda_1 0 \lambda_1 00$	$\lambda_1 0 \lambda_2 00$	$\lambda_1 0 \lambda_3 00$	$\lambda_1 0 \lambda_4 00$	$\lambda_1 0 \lambda_0 00$
$\lambda_2 0 \lambda_2 00$	$\lambda_2 0 \lambda_3 00$	$\lambda_2 0 \lambda_4 00$	$\lambda_2 0 \lambda_0 00$	$\lambda_2 0 \lambda_1 00$
$\lambda_3 0 \lambda_3 00$	$\lambda_3 0 \lambda_4 00$	$\lambda_3 0 \lambda_0 00$	$\lambda_3 0 \lambda_1 00$	$\lambda_3 0 \lambda_2 00$
$\lambda_4 0 \lambda_4 00$	$\lambda_4 0 \lambda_0 00$	$\lambda_4 0 \lambda_1 00$	$\lambda_4 0 \lambda_2 00$	$\lambda_4 0 \lambda_3 00$

Table 2
Mlmw-oocs Long Codeword 1000000100, 5 Wavelengths, Code Weight 2, Code Length 10.

Group 0	Group 1	Group 2	…	Group 4
$\lambda_0 000000 \lambda_0 00$	$\lambda_0 000000 \lambda_1 00$	$\lambda_0 000000 \lambda_2 00$	…	$\lambda_0 000000 \lambda_4 00$
$\lambda_1 000000 \lambda_1 00$	$\lambda_1 000000 \lambda_2 00$	$\lambda_1 000000 \lambda_3 00$	…	$\lambda_1 000000 \lambda_0 00$
$\lambda_2 000000 \lambda_2 00$	$\lambda_2 000000 \lambda_3 00$	$\lambda_2 000000 \lambda_4 00$	…	$\lambda_2 000000 \lambda_1 00$
$\lambda_3 000000 \lambda_3 00$	$\lambda_3 000000 \lambda_4 00$	$\lambda_3 000000 \lambda_0 00$	…	$\lambda_3 000000 \lambda_2 00$
$\lambda_4 000000 \lambda_4 00$	$\lambda_4 000000 \lambda_0 00$	$\lambda_4 000000 \lambda_1 00$	….	$\lambda_4 000000 \lambda_3 00$

Table 3
Examples of the Mlmw-oocs with different lengths.

w	m	(code length, cardinality) of each length	Φ
2	5	(5,25), (10,50)	75
3	3	(19,18), (247,117)	135
4	4	(25,16), (425,272)	288
4	6	(25,36), (275,396)	432
4	8	(25,64), (125,320)	384

As a general rule, the code weight of the MLMW-OOCs is subject to $w \leq m$. In [24], an algebraic construction algorithm is proposed, which is done by expanding 1D single-wavelength multiple length OOCs into MLMW-OOCs, while maintaining the correlation properties, i.e., these constructed codewords have auto- and cross-correlation values of both at most one.

Here, we introduce this algebraic construction algorithm to only design the simplified double-length MLMW-OOCs for PON fiber link monitoring. It is because that more different-length (more than two) cases will have more complex interfering patterns and hence the hit probabilities become hard to calculate. Thus, we consider a set of code lengths is $F = \{F_s, F_l\}$, where F_s and F_l are the code length of the short and long codewords, respectively. To obtain a good autocorrelation peak and faintish cross-correlation spikes, we assume that the autocorrelation constraints $\lambda_a = \{1, 1\}$ and the cross-correlation constraints $\lambda_c = \{1, 1, 1\}$, respectively. The number of the short codewords and the long codewords are assumed to be Φ_s and Φ_l, respectively. Thus the code cardinality of the double-length MLMW-OOCs is $\Phi = \Phi_s + \Phi_l$, and the codeword-cardinality distribution ratio is $D = \{\Phi_s/\Phi, \Phi_l/\Phi\}$. It is worth noting that the number of the short codewords is smaller than that of the long codewords for the double-length MLMW-OOCs, i.e., $\Phi_s < \Phi_l$, according to the adopted codeword construction method.

Example of the double-length MLMW-OOC Construction: An algebraic construction of a new class of MLMW-OOCs with both the auto-correlation and cross-correlation values of at most one was researched in [24]. One can first recursively construct 1D time-spreading multiple-length OOCs and then extend this 1D-OOCs into the MLMW-OOCs following the procedure in [24]. For instance, as shown in Tables 1 and 2, we first construct two 1D-OOCs codewords (10100 and 1000000100) with different code lengths (5 and 10) and then expand these two 1D-OOCs into MLMW-OOCs respectively, in which the number of wavelengths is 5 and code weight is 2. Using this construction method, a variety of the MLMW-OOCs with different coding parameters can be designed in Table 3. A (6×{25, 275}, 4, {1, 1}, {1, 1, 1}, {36/432, 396/432}) double-length MLMW-OOC with 6 wavelengths is constructed in Table 3, where the code weight is 4, the number of short codewords is 36 with the code length of 25, the number of long codewords is 396 with the code length of 275, respectively. The number of the short codewords is smaller than that of the long codewords. These double-length codewords can be used for the optical coding monitoring system in a high-capacity PON, to further reduce the inter-user interferences.

One-hit Probability Analysis: In an O-CDMA system, the one-hit probability of each user with the single-length OOCs is traditionally assumed identical [25]. But, with the MLMW-OOCs in use, the hit probability of a user depends on the length of target codeword as well as the length of the interfering codewords. There are two cases to be considered for a given target codeword: (1) the interference comes from the same length codewords, or (2) comes from the different length codewords. The probabilities of obtaining one hit between two OOCs have been discussed in [26]. In this paper, the probability of getting one hit between the double-length codewords can be also obtained using the similar methods. The coding parameters are modified correspondingly to satisfy the optical coding monitoring requirements [24].

First case, the probability of obtaining one hit between two same-length short codewords is given by

$$q_s = \frac{mw^2(m\Phi_s - 1) + (m-1)(w-1)^2}{mF_s(m^2\Phi_s - 1)}. \tag{1}$$

Likewise, the probability of obtaining one hit between two same-length long codewords is

$$q_l = \frac{mw^2(m\Phi_l - 1) + (m-1)(w-1)^2}{mF_l(m^2\Phi_l - 1)}. \tag{2}$$

Second case, if the target codeword is short and the interfering one is long, the probability of obtaining one hit can be derived as

$$q_{s,l} = \frac{mw^2(m\Phi_l - 1) + (m-1)(w-1)^2}{mF_l(m^2\Phi_l - 1)}. \tag{3}$$

Similarly, the probability of obtaining one hit between the target long codeword and the interfering short codeword can be obtained as

$$q_{l,s} = \frac{mw^2(m\Phi_s - 1) + (m-1)(w-1)^2}{mF_s(m^2\Phi_s - 1)}. \tag{4}$$

Note that the performance of optical coding monitoring system is limited by the interferences coming from other branches [8,11]. Hence, the one-hit probability is an important parameter for the SIR performance analysis. To obtain the detailed derivation process, the readers can refer to [24].

3.2. Principle of MLMW-OOC-based monitoring system

The schematic diagram of the MLMW-OOC-based fiber fault in-service monitoring system is shown in Fig. 1. At the OLT, the broadband light source (BBS) generates a U-band detecting pulse with the power of P_S and the duration of T_C, which is combined with up-/down-stream (US/DS) data signals in C-band by using a wavelength division multiplexer (WDM). The detecting pulse is transmitted through a circulator and a section of feeder fiber (FF) to a remote node (RN), where it is split into N sub-pulses by a 1: N passive splitter. Every sub-pulse travels through DDF to the front end of the corresponding ONU and then it is encoded into a sub-pulse sequence by the optical encoder. It is noted that the encoder is transparent to C-band data signals, and only reflects the encoding signals in U-band back to the monitoring system at the OLT.

As shown in Fig. 1, for monitoring each DDF link, unique MLMW-OOC codeword is assigned to the corresponding optical encoder at the edge of the DDF, according to our proposed assignment scheme. Thus, given a PON with N DDF branches, the N passive MLMW-OOC encoders with the different codewords are required to be installed at the edge of the DDFs to identify respective branches, which is made of a MFBG with low cost and simple fabrication. Each FBG of the encoder can reflect a different wavelength in a specific time (i.e., discrete position), which corresponds to a preset 2D MLMW-OOC codeword.

In monitoring system, the return encoding signal of each DDF branch is decoded by auto-correlation operation with the corresponding

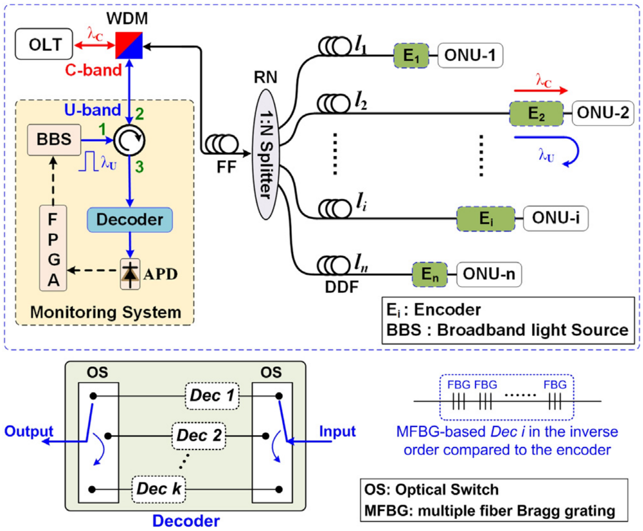

Fig. 1. The schematic diagram of the MLMW-OOC-based fiber fault in- service monitoring system for high-capacity PONs. The implementation of the decoder using OS and MFBG is also shown for auto-correlation operation.

MLMW-OOC optical decoder. The optical decoder is implemented by using two optical switches (OS) and N sub-decoders as shown in Fig. 1. Each sub-decoder is also made of a MFBG but in reverse order compared to its corresponding encoder. Note that the concrete configuration of the optical decoder depends on the total number (i.e., N) of the DDF branches to be monitored and the adopted type of the 2D codewords. Since the user geographical distribution is fixed, there is no need to change the codewords assigned to all the DDF customers, according to the proposed assignment scheme. Depending on the target DDF to be monitored, the OS selects the corresponding sub-decoder, i.e., one DDF is monitored at a time. Hence, one avalanche photodiode (APD) is sufficient for the monitoring system, which converts the auto-correlation optical signal obtained from the sub-decoder into electrical signal. As the different MLMW-OOC codewords are assigned to each DDF, the corresponding detected electrical signal is further processed with the field programmable gate array (FPGA) board to assess the status of the individual fiber link. If all the fiber links (FF and DDFs) works well, the detected signal (i.e., an auto-correlation peak) for the target link should exist. Otherwise, a missing monitoring signal indicates a failure. If a fiber break occurs in the FF, no monitoring signal is observed for any DDF. Note that the fiber fault monitoring scheme only provides information on assessing fiber link status, i.e., faulty (with a break) or healthy (with no break), rather than evaluating the monitoring signal quality. The fault location is another important issue, but outside of the scope of this paper.

But when an additional ONU is newly-added physically, we need to choose an unused codeword available from the code space (i.e., code cardinality), and assign it to this new DDF link for monitoring. Meanwhile, a new encoder is required to be installed placed at the edge of the new DDF, and a sub-decoder is added in the “Decoder” module of the monitoring system as shown in Fig. 1. In the case that great changes occur in the PON configuration (e.g., multiple new ONUs are added in the PON), it should be better that all DDF links are re-assigned with new codewords by using our proposed assignment scheme, to obtain better system SIR performance. Thus, the new encoders are equipped in those newly-added DDF links, while the original encoders should be updated with the new codewords. The “Decoder” module of the monitoring system located in the CO should be also updated by replacing all new sub-decoders.

Note that significant differences would exist between the standard O-CDMA system and the optical-coding-based link monitoring system

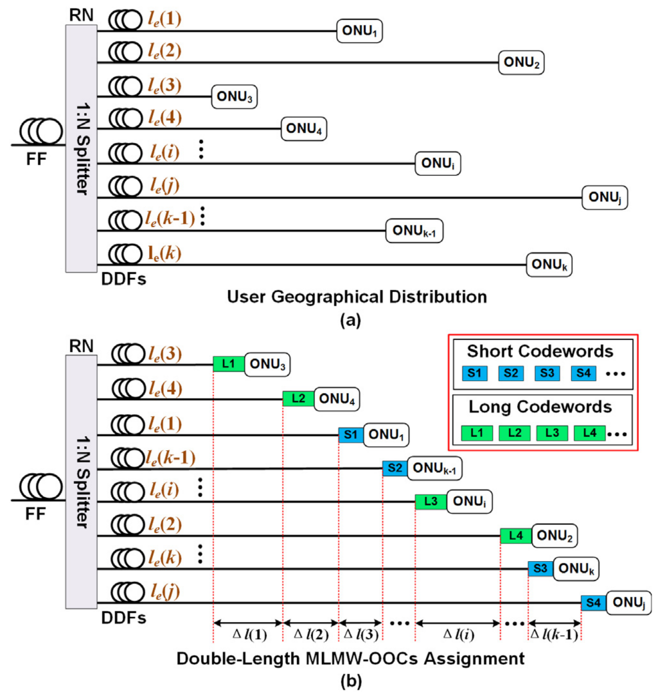

Fig. 2. The schematic diagram of (a) user geographical distribution in PON; (b) double-length MLMW-OOC assignment scheme.

in PONs. In standard O-CDMA systems, the MLMW-OOCs with both the auto-correlation λ_a and the cross-correlation λ_c values of more than one are constructed and the codewords with the different code lengths are assigned to the different demands, in order to support multi-rate transmission and quality-of-services (QoS) services [24–28]. But, in the link monitoring system, no data information needs to be transmitted in the U-band. The interferences are merely related to the monitoring channels and have nothing to do with the data channels in the C-band. In this paper, we utilize the simplified double-length (i.e., short and long code lengths) MLMW-OOCs for monitoring fiber links in a high-capacity PON to reduce the effect of inter-user interference with our proposed codeword assignment scheme. Moreover, because the length of the FBG encoder depends on the length of codeword generated, the shorter codewords are preferred in our codeword assignment scheme, and thus the adopted FBG encoders have a relative shorter length and lower fabrication cost.

4. Double-length MLMW-OOC assignment scheme based on user geographical distribution

4.1. Proposed codeword assignment scheme

In the existing fixed-length 2D-OOC-based PON monitoring schemes [8,11], all the codewords have *identical code length* and are *assigned randomly* to users without the consideration of the user geographical distribution information. Hence, there exist severe interferences especially if the user separation lengths (i.e., the lengths of DDFs) are close to each other. Furthermore, with the increase of the network size, the lengths of the required codewords become abnormally large. To solve this issue, we propose an assignment scheme of the double-length MLMW-OOCs by considering the user geographical distribution. As illustrated in Fig. 2(a), the deployment of ONUs is distributed within a certain distance and some users may be close to each other in distance. The main idea behind our assignment scheme is to prioritize the short codewords to those users that are close to each other in distance. Note that the OLT can automatically learn the RTT data for each newly- connected ONU via the ranging process in the auto-discovery mechanism [1]. Thus the physical distance of each ONU (i.e., the length of DDF) is known, which could not induce any burden for access network operators.

The procedure of the assignment scheme is as follows:

(1) Construct a class of the double-length MLMW-OOCs codewords according to the method mentioned above in the Section 3.1. We assume that the numbers of the short codewords and the long codewords are Φ_s and Φ_l, and hence the code cardinality $\Phi = \Phi_s + \Phi_l$. The network size (i.e., the number of users) is fixed to be K. The number of the assigned short and long codewords in the monitoring system is K_s and K_l, and the constraint conditions are $K = K_s + K_l$, $K \le \Phi$, $K_s \le \Phi_s$ and $K_l \le \Phi_l$, respectively. Let l_e be the maximum client separation length (i.e. the maximum length of the DDF). Thus, each length of the DDFs is assumed to be distributed uniformly in $[0, l_e]$.

(2) Set $\{l_e(1), l_e(2), l_e(3), l_e(4), \ldots, l_e(i), l_e(j), \ldots, l_e(k-1), l_e(k)\}$ to the lengths of k DDFs as shown in Fig. 2(a), respectively; Sort these user separation lengths in an ascending order, such as $\{l_e(3), l_e(4), l_e(1), l_e(k-1), \ldots, l_e(i), l_e(2), \ldots, l_e(k), l_e(j)\}$ in Fig. 2(b).

(3) Calculate the distance difference Δl of two adjacent lengths of DDFs as follows

$$\Delta l(1) = l_e(3) - l_e(4),$$

$$\Delta l(2) = l_e(4) - l_e(1),$$

$$\Delta l(3) = l_e(1) - l_e(k-1),$$

$$\ldots$$

$$\Delta l(i) = l_e(i) - l_e(2),$$

$$\ldots$$

$$\Delta l(k-1) = l_e(k) - l_e(j).$$

(4) Sort these distance differences Δl in an ascending order: such as $\Delta l(3) \le \Delta l(k-1) \le \cdots \le \Delta l(2) \le \Delta l(1) \le \Delta l(i) \le \cdots$.

(5) According to the Δl sorting above, the pair of users with the minimum Δl will be given priority in allocation of the short codewords, and then the other user pairs are assigned in turn until all short codewords run out. Then the long codewords are assigned for remaining users.

There is a special case if two or more ONUs are at the same distance from the OLT. In the case, the distance difference Δl of these ONUs with the same length of DDFs is zero. Thus these ONUs are given the highest priority in allocation of short codewords, according to our assignment scheme. Moreover, due to the fact that unique MLMW-OOC codeword is assigned to the different encoders installed at the edge of the DDFs, these different DDF branches can be identified well.

Note that the user geographical distribution characteristics (i.e., the distance differences Δl between users) would strongly affect the interference statistics. It is because that there may exist severe interferences when the difference Δl of user separation length is within the correlation distance l_{CD}. With our proposed double-length MLMW-OOC assignment scheme, those users close to each other in distance are assigned with the short codewords preferentially. These short codewords have the shorter code length, and hence have smaller inter-code interference. In the following, we will analyze mathematically how the assignment scheme can affect the SIR performance of this monitoring system.

4.2. Signal-to-interference ratio analysis

As we know, the length of a codeword sequence is expressed to be $c{\times}FT_C/2$, where c is the speed of light in the fiber, $F = \{F_s, F_l\}$ is a set of the code lengths of the short or long codeword, T_C is the pulse duration time. As shown in Fig. 3(a), the length of the encoder $(F-1) \times T_C$ plus is merely the interval length between the first and the last sub-pulses in a codeword sequence. Hence, the codeword length is also the length of the encoder plus one pulse duration T_C. The $l_i = l_{FF} + l_{DDFi}$ is total length from the ONU$_i$ to the OLT, including the FF and a piece of DDF$_i$. Thus, the distance difference of the two branches is assumed to be Δl ($\Delta l > 0$). When the $\Delta l = |l_i - l_1|$ between the target encoder E_1 and another encoder E_i is smaller than the $c{\times}FT_C/2$, the encoded signal reflected by the E_i will partially overlap with the target codeword signal, which will contribute to the partial interference. On the contrary, if the $\Delta l = |l_2 - l_1|$ between E_2 and E_1 is larger than the $c{\times}FT_C/2$, it indicates that the two codeword signals cannot overlap with each other and hence there exist no interference. Therefore, for any short or long target codeword signal, the correlation distance is calculated as follows

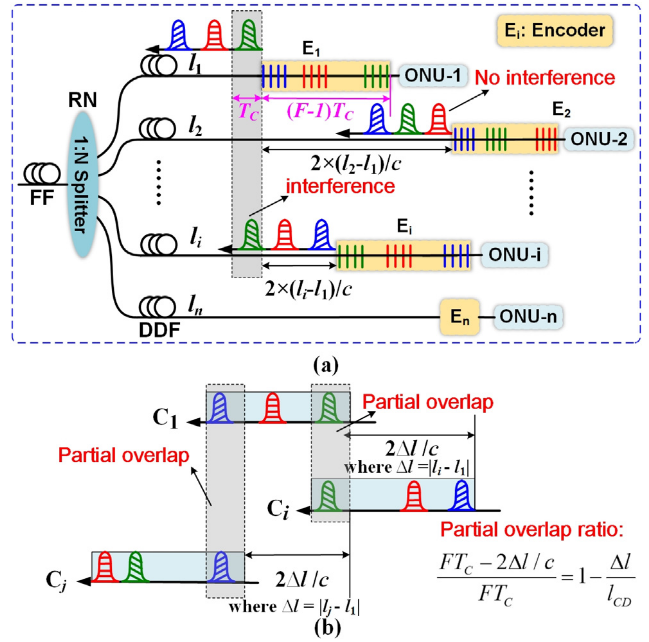

Fig. 3. (a) Principle of the correlation distance; (b) the partial interference between C_i or C_j and the target C_1, respectively.

$$l_{CD,j} = \frac{c \times F_j T_C}{2}, j \in \{s, l\}. \tag{5}$$

In the MLMW-OOC-based monitoring system, due to the different lengths of DDFs, any two codewords (i.e., monitoring signals) from the different branches would partially overlap in the time domain as shown in Fig. 3(b). Therefore, the partial interference ratio ρ_j between the target codeword signal and the interference signal can be defined as follow.

$$\rho_j = \frac{F_j T_C - 2\Delta l/c}{F_j T_C} = 1 - \frac{\Delta l}{l_{CD,j}}, j \in \{s, l\}. \tag{6}$$

In previous works [8–10], the system mathematical model for the 2D-OOCs with the random assignment scheme has been established. Based on the model, we can further derive the mathematical expressions of the SIR for the MLMW-OOCs with our proposed codeword assignment scheme.

Firstly, the expression of the desired target signal (i.e., an autocorrelation peak) is same as that in the existing models [8–10], which can be expressed as

$$\mu_{sig,j} = G\alpha_{Total}\xi_i e^{-2\alpha_a l_{i,j}} w P_S, j \in \{s, l\}. \tag{7}$$

where G is the gain of the APD, α_{Total} denotes the total losses including the circulator, splitter, connectors, and so forth, in the monitoring system. $\xi_i \in \{0, 1\}$means the different status of the target DDF$_i$. Specifically, if the DDF$_i$ is broken, $\xi_i = 0$. When the DDF$_i$ is healthy, $\xi_i = 1$. And the detection pulse can be encoded into a sub-pulse sequence in the optical domain and reflected back to the OLT. The term $e^{-2\alpha_a l_{i,j}}$ is an attenuation model for the FF and DDFs, where α_a is the fiber attenuation coefficient. P_S is the power of the MLMW-OOC signal with w sub-pulses. From Eq. (7), we can find that no matter the target signal has the short or long codeword length, the desired target signal has the same expression, because of the same code weight w.

Under the constraints $K = K_s + K_l$, $K \le \Phi$, $K_s \le \Phi_s$ and $K_l \le \Phi_l$, we considered two specific cases. (i) When the target codeword is short, the interfering codeword length can be either short or long. Thus, the interference components consists of two parts, which can be written as

$$\mu_{int,s} = G\alpha_{Total}\xi_k\rho_s\left[\left(K_s-1\right)q_s e^{-2\alpha_a l_{k,s}} + K_l q_{s,l} e^{-2\alpha_a l_{k,l}}\right]P_S. \tag{8}$$

Similarly, (ii) if the target codeword is long, the interfering codeword length can be either short or long. Thus the interference components can be also expressed as

$$\mu_{int,l} = G\alpha_{Total}\xi_k\rho_l\left[\left(K_l-1\right)q_l e^{-2\alpha_a l_{k,l}} + K_s q_{l,s} e^{-2\alpha_a l_{k,s}}\right]P_S. \tag{9}$$

Then, for the short or long target codeword signal, the SIR_j is defined as the square of the expectation of the desired signal power divided by the expectation of the power of the interference components, as shown in Eq. (10).

$$\mathrm{SIR}_j \overset{def}{=} \left[\frac{E(\mu_{sig,j})}{E(\mu_{int,j})}\right]^2, j \in \{s,l\}. \tag{10}$$

Using Eqs. (5)–(10), we can derive the detailed expression of the SIR as shown in Eqs. (11) and (12) (see the equations in Box I). Eq. (11) is the SIR_s when the target codeword is short; Eq. (12) is the SIR_l when the target codeword is long. We assume the length of target fiber link is l_1 and the length of interfering fiber link is l_2, hence the distance difference $\Delta l = |l_2 - l_1|$. To calculate the conditional expectation value in Eqs. (11) and (12), we assume that l_e is the maximum client separation length (i.e. the maximum length of DDFs). Then the length l_k of each DDF_k is distributed uniformly in $[0, l_e]$. We can vary the values of l_e and the network size K to simulate the different client density. When the value of l_e is a smaller and K is larger, the client density is larger, and vice versa. Let $p(l_k)$ be the probability density function (PDF) of the length l_k of the DDF_k, which is assumed to be independent identically distributed (IID). Hence, the target fiber link l_1 is at the interval $[l_f, l_f + l_e]$, where l_f is the FF length. As discussed in Section 2.3, the user geographical distribution will strongly affect the interference statistics. Thus if the link $l_2$satisfies the constraint $|l_2 - l_1| \le l_{CD}$, the return codeword signal from the link l_2 will cause the undesired interference. More specifically, we can obtain the expression as follows

$$Max\left(l_f, l_1 - l_{CD,j}\right) \le l_2 \le Min\left(l_f + l_e, l_1 + l_{CD,j}\right), j \in \{s,l\}. \tag{13}$$

Thus, the interference ratio can be further expressed to be

$$\frac{\left|Min\left(l_f + l_e, l_1 + l_{CD,j}\right) - Max\left(l_f, l_1 - l_{CD,j}\right)\right|}{l_e}, j \in \{s,l\}. \tag{14}$$

Finally, we can get the total SIR of the monitoring system as follow

$$\mathrm{SIR} = \frac{K_s}{K}\cdot\mathrm{SIR}_s + \frac{K_l}{K}\cdot\mathrm{SIR}_l, (K = K_s + K_l). \tag{15}$$

In the following simulation, the SIR is an important metric to be evaluated for the optical-coding-based monitoring system.

5. Performance evaluation

In the simulations, to assess the performance of our proposed double-length MLMW-OOC-based link monitoring system, we compared it with the 2D-OOC-based coding monitoring system in our developed matlab simulation platform. The family of (F, m, w, λ_a, λ_c) are traditionally used to describe 2D-OOCs, where F=$Kw(w-1)$+1 is the code length, m is the number of wavelengths, w is the code weight, $\lambda_a = 1$ represents the maximum auto-correlation side lobe, and $\lambda_c = 1$ represents the

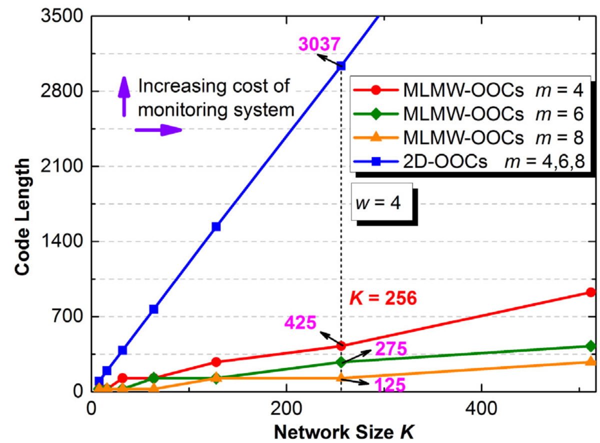

Fig. 4. Code length versus network size for the MLMW-OOC and 2D-OOC coding schemes with code weight $w = 4$ and different wavelengths m. Code length denotes the number of bits in a code, and thus it has no unit.

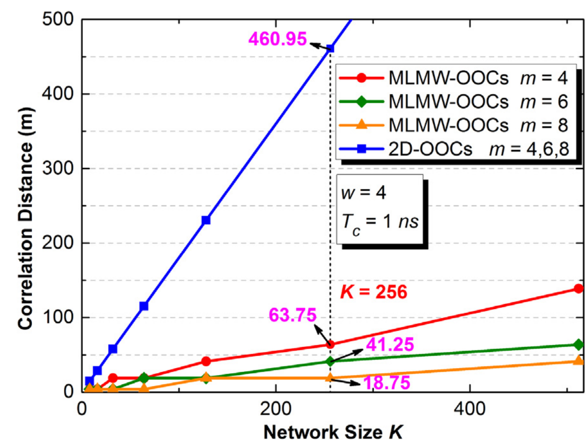

Fig. 5. Correlation distance versus network size for the MLMW-OOC and the 2D-OOC coding schemes with $w = 4$, $T_C = 1$ ns and different wavelengths m.

maximum cross-correlation value [8,11]. We consider the transmitted pulse power $P_S = 4$ dBm in order not to induce fiber nonlinearity, because that the linear monitoring system is no longer stable for a higher power. In addition, the detecting pulse width T_C is assumed to be 1 ns and 0.3 dB/km fiber loss is assumed for an U-band broadband light source. In our previous work [11], we have found that the optimal pulse width T_C is set to be 1 ns according to a trade-off between the detection noises and the interferences. An APD with gain of 100 is used and total loss is 5 dB for the circulator, splitter, connectors, etc. We consider a 20 km FF link between the OLT and RN.

5.1. Code characteristic comparison and analysis between MLMW-OOCs and 2D-OOCs

We first study the code characteristics between the MLMW-OOCs and the 2D-OOCs with the different wavelengths. In Fig. 4, we plot the code length versus the consumer network size K for the two coding schemes in the case of the code weight $w = 4$. We can observe that the required code length becomes large as the network size K increases for both of the two coding schemes. For a given user network size $K = 256$, the code length of the 2D-OOCs reaches up to impractical 3037, which is much longer than that of the MLMW-OOCs. It means that the optical encoder (i.e., multi-FBG) length of the MLMW-OOCs is much shorter than that of the 2D-OOCs. Thus, it would significantly decrease the CAPEX of the proposed monitoring system, especially for high-capacity PONs with the

$$\sqrt{\mathrm{SIR}_s} = \frac{w\cdot E\left\{e^{-2\alpha_a l_1}\right\}}{\left[\left(K_s-1\right)q_s + K_l q_{s,l}\right]\cdot E_{l_1}\left\{E_{l_2/l_1}\left\{\rho_s e^{-2\alpha_a l_2}|l_1\right\}\right\}}$$
$$= \frac{w\int_{l_f}^{l_f+l_e} p(l_1)e^{-2\alpha_a l_1}dl_1}{\left[\left(K_s-1\right)q_s+K_lq_{s,l}\right]\cdot\int_{l_f}^{l_f+l_e}p(l_1)\int_{\max(l_f,l_1-l_{CD,s})}^{\min(l_f+l_e,l_1+l_{CD,s})}\frac{\left|\min(l_f+l_e,l_1+l_{CD,s})-\max(l_f,l_1-l_{CD,s})\right|}{l_e}\cdot\left(1-\frac{\Delta l}{l_{CD,s}}\right).p(l_2)e^{-2\alpha_a l_2}dl_2dl_1}. \tag{11}$$

$$\sqrt{\mathrm{SIR}_l} = \frac{w\cdot E\left\{e^{-2\alpha_a l_1}\right\}}{\left[\left(K_l-1\right)q_l + K_s q_{l,s}\right]\cdot E_{l_1}\left\{E_{l_2/l_1}\left\{\rho_l e^{-2\alpha_a l_2}|l_1\right\}\right\}}$$
$$= \frac{w\int_{l_f}^{l_f+l_e} p(l_1)e^{-2\alpha_a l_1}dl_1}{\left[\left(K_l-1\right)q_l+K_sq_{l,s}\right]\cdot\int_{l_f}^{l_f+l_e}p(l_1)\int_{\max(l_f,l_1-l_{CD,l})}^{\min(l_f+l_e,l_1+l_{CD,l})}\frac{\left|\min(l_f+l_e,l_1+l_{CD,l})-\max(l_f,l_1-l_{CD,l})\right|}{l_e}\cdot\left(1-\frac{\Delta l}{l_{CD,l}}\right).p(l_2)e^{-2\alpha_a l_2}dl_2dl_1}. \tag{12}$$

Box I.

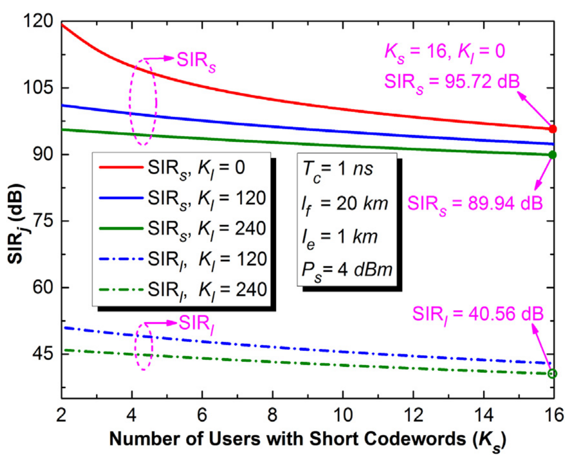

Fig. 6. SIR_s and SIR_l versus the short codewords K_s in the case of the different numbers long codewords K_l of the double-length MLMW-OOCs.

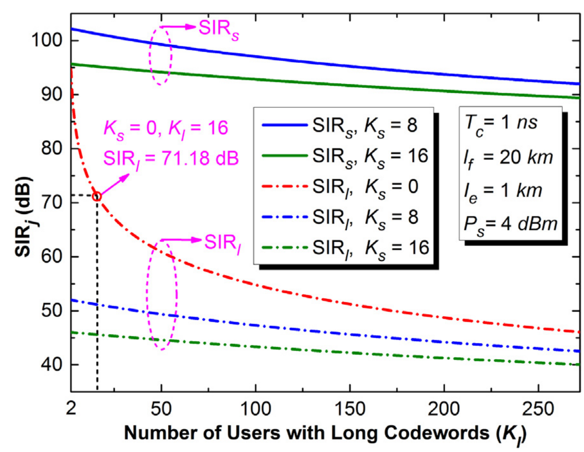

Fig. 7. SIR_s and SIR_l versus the long codewords K_l under the different numbers of short codewords K_s of the double-length MLMW-OOCs.

larger consumer network size K (i.e., the number of users). From Fig. 4, we also find that when the $K = 256$, by using the constructed MLMW-OOC codewords as shown in Table 3, as the number of wavelengths m increases, the code length of the MLMW-OOCs gets shorter. It is because that the larger number of wavelengths will greatly increase the code capacity, and thus decrease the corresponding code length. Hence, our proposed scheme can support the monitoring of high-capacity PONs with the shorter code length and the lower cost. It makes our proposed scheme more feasible in practice deployment.

In Fig. 5, we present the correlation distance for the MLMW-OOC and the 2D-OOC coding schemes in the case of the different network sizes. As shown in Eq. (5), the correlation distance is linearly proportional to the code length. Hence the correlation distance becomes larger and larger as the different network size K increases for both of the two coding schemes. Moreover, the correlation distance of the MLMW-OOCs is much smaller than that of the 2D-OOCs. When the client network size $K = 256$ and the number of wavelengths is 4, the correlation distance of MLMW-OOCs is 63.75 m, which is remarkably smaller than 460.95 m with the 2D-OOCs. As the number m of wavelengths increases, the correlation distance of the MLMW-OOCs will go lower. As discussed in Section 2.4, the smaller the correlation distance is, the smaller the partial interference ratio becomes. Particularly, there is no interference when the distance difference Δl between the target and the interfering links is out of the range of the correlation distance of the target link. Therefore, our proposed monitoring scheme based on the MLMW-OOCs can support high capacity PONs with the smaller correlation distance and hence the lower inter-user interferences.

5.2. Relationship between SIR_s and SIR_l for MLMW-OOCs

Using the MLMW-OOCs construction method mentioned in Section 2.2, an (4×{25, 425}, 4, {1, 1}, {1, 1, 1}, {16/192, 272/288}) double-length MLMW-OOCs with 4 wavelengths are designed. There are 16 short codewords with the code length of 25, and 272 long codewords with the code length of 425. In Fig. 6, when $T_C = 1$ ns, $l_f = 20$ km, $l_e = 1$ km and $P_S = 4$ dBm, we give out the SIR_s and SIR_l curves versus the short codewords K_s in the case of the different numbers of long codewords K_l of the double-length MLMW-OOCs. The solid curves depict the performance of SIR_s as expressed in Eq. (11), the dash-dotted curves correspond to the performance of SIR_l as expressed in Eq. (12). In Fig. 6, for each curve with a given number of the long codewords K_l, the performance of both SIR_s and SIR_l decreases with the number of short codewords K_s increases. For different curves with the different K_l, when the K_l increases, both the SIR_s and SIR_l become worsen. It is because that the increase of the total number of users $K = K_s + K_l$ will worsen the SIR performances (refer to the numerator of Eqs. (11) and (12). The solid curve with $K_l = 0$ shows that when there is no long codeword, the SIR_s of the MLMW-OOCs presents the highest value. We can also observe that the SIR_s always performs much better than the SIR_l. It is explained by the fact that users assigned with the short codewords always perform better than those assigned with the long codewords, due to the shorter correlation distance and the lower interference ratio. For example, we assume that the total number of users $K = K_s + K_l$ is 256 in a PON, while $K_s = 16$ and $K_l = 240$. We can find that the SIR_s of 89.94 dB is larger than the SIR_l of 40.56 dB.

Using the same simulation conditions, we plot SIR_s and SIR_l versus the long codewords K_l under the different numbers of the short codewords K_s as shown in Fig. 7. The solid curves and dash-dotted curves represent the SIR_s and SIR_l, respectively. Similarly, the SIR_s performance for the users assigned with the short codewords is always better than the SIR_l for those assigned with the long codewords, due to the same reason (i.e., shorter correlation distance and the lower interference ratio). For different curves with the different K_s, the SIR_s and SIR_l decrease as the K_s increases, because the total number of users $K = K_s + K_l$ increases. Overall, both SIR_s and SIR_l decrease as the total number of users $K = K_s + K_l$ increases, because that the total interferences increase. The dash-dotted curve with $K_s = 0$ represents the SIR_l of MLMW-OOCs with the long codewords only. For instance, for a PON with 16 users, when the $K_s = 16$ and $K_l = 0$ in Fig. 6, the users only assigned with the short codewords have the SIR_s performance of 95.72 dB, which is larger than the SIR_l of 71.18 dB when the users only assigned with the long codewords ($K_s = 0$ and $K_l = 16$ in Fig. 7).

5.3. SIR comparison between MLMW-OOCs and 2D-OOCs under different network sizes and client separation lengths

From what has been discussed above, we conclude that users assigned with short codewords always perform better than those assigned with long codewords. In our proposed double-length MLMW-OOC assignment scheme (refer to Section 2.3), the short codewords are preferentially assigned to those users who are close to each other in distance. To demonstrate the advantages of the proposed codeword assignment scheme, we compare it with the random codeword assignment scheme of the 2D-OOCs. In our previous work [11], the SIR performance of 2D-OOC-based scheme has been studied. Here, as expressed in Eq. (15), the SIR of the MLMW-OOC-based monitoring system is derived. We consider different client separation length $l_e = 1$ km and $l_e = 2$ km to simulate different client density. For a fixed network size K, the smaller the value of l_e is, the higher the client density is, and vice versa. Moreover, we assume that $T_C = 1$ ns, $l_f = 20$ km, $P_S = 4$ dBm, and $w = 4$, respectively. In the following simulations, we vary the different numbers of the MLMW-OOCs and the different number of wavelengths m.

Using the above simulation conditions and $m = 4$, in Fig. 8(a) we plot the SIR curves for the MLMW-OOC and 2D-OOC coding schemes in the case of different network sizes K and different client separation lengths l_e, where solid and dash-dotted curves represent the MLMW-OOC and 2D-OOC coding schemes, respectively. As a whole, the performance worsens as the network size K increases due to the increase of the interference. In Fig. 8(a), for a given network size $K = 256$, when $l_e = 1$ km, we can find that the SIR of MLMW-OOCs is 46.58 dB, which is larger than 32.34 dB of 2D-OOCs; when $l_e = 2$ km, the SIR of MLMW-OOCs is 58.45 dB, which is also larger than 42.59 dB of 2D-OOCs. Therefore, we can conclude that the SIR of the MLMW-OOCs is always higher than the 2D-OOCs under different client separation lengths. In addition, for a fixed K, as the client separation length l_e increases from 1 km to 2 km, the SIR performances of the MLMW-OOCs and the 2D-OOCs can improve from 46.58 dB to 58.45 dB and from 32.34 dB to 42.59 dB, respectively. It is because that the distance difference Δl of two adjacent users increases, which leads to the decrease of interference signal.

We also give out the SIR versus network size K for $m = 6$ and $m = 8$ in Figs. 8(b) and 8(c), respectively. For a given network size $K = 256$, while the m is 6 and 8, the number of short codewords K_s is 36 and 64, the SIR increases as assigned K_s (the number of short codewords) increases. In addition, as m increases, the SIR improvement of the MLMW-OOCs is better than that of the 2D-OOCs. As a whole, we can conclude from both figures that the performance of the MLMW-OOCs performs better than the 2D-OOC coding scheme.

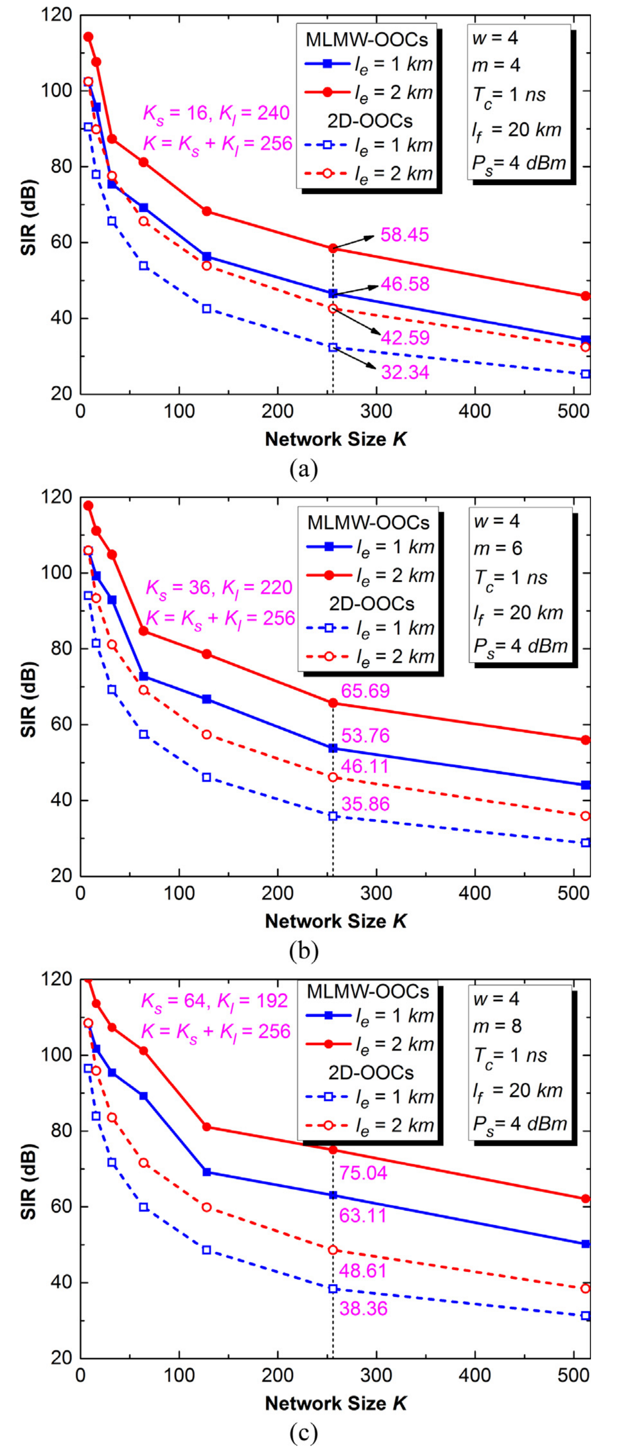

Fig. 8. SIR versus network size K for double-length MLMW-OOC and 2D-OOC coding schemes with different client separation length l_e, $T_C = 1$ ns, $l_f = 20$ km, $P_S = 4$ dBm, $w = 4$ and (a) $m = 4$; (b) $m = 6$; (c) $m = 8$.

6. Conclusion

Cost-effective, in-service fault monitoring of fiber links in a high-capacity PON is becoming increasing important for network operators. Different from the existing OC-based monitoring schemes, a novel codeword assignment scheme based on the double-length MLMW-OOCs is proposed in this paper, with the consideration of the user geographical distribution. For the MLMW-OOC-based monitoring scheme, the new parameter "interference ratio" is defined and the mathematical expression of the SIR is given out in a more precise way. In the extensive simulations, we evaluated the code characteristics in terms of the code length and the correlation distance for both the MLMW-OOC and 2D-OOC coding schemes. Also, we evaluated the SIR performances versus network size K for the double-length MLMW-OOC and 2D-OOC coding schemes with different use separation lengths and wavelengths. The simulation results show that compared to the 2D-OOC coding scheme, our proposed scheme can support the monitoring of high-capacity PONs with shorter code length to reduce cost and smaller correlation distance to reduce interference, and better SIR performance. The two nice features make the novel scheme more feasibility and superiority.

Acknowledgment

The work was supported by the National Natural Science Foundation of China (NSFC) (61771134).

References

[1] H.S. Abbas, M.A. Gregory, The next generation of passive optical networks: A review, J. Netw. Comput. Appl. 67 (2016) 53–74.
[2] J. Montalvo, A. Tapetado, D.S. Montero, C. Vázquez, New fiber supervision technique for passive optical networks supporting mobile services, IEEE Photon. Technol. Lett. 28 (4) (2016) 501–504.
[3] X. Long, C. Xiaofei, X. Zhaowen, H. Qirui, Lengthened simplex codes with complementary correlation for faulty branch detection in TDM-PON, IEEE Photon. Technol. Lett. 25 (23) (2013) 2315–2318.
[4] M.M. Rad, K. Fouli, H.A. Fathallah, L.A. Rusch, M. Maier, Passive optical network monitoring: Challenges and requirements, IEEE Commun. Mag. 49 (2) (2011) S45–S52.
[5] H. Fathallah, L.A. Rusch, Code division multiplexing for in-service out-of-band monitoring of live FTTH-PONs, J. Optical Netw. 6 (7) (2007) 819–829.
[6] M.M. Rad, H. Fathallah, S. LaRochelle, L.A. Rusch, Computationally efficient monitoring of PON fiber link quality using periodic coding, IEEE/OSA J. Opt. Commun. Netw. 3 (2011) 77–86.
[7] M. Rad, J. Penon, H. Fathallah, S. LaRochelle, L. Rusch, Probing the limits of PON monitoring using periodic coding technology, IEEE J. Lightw. Technol. 29 (9) (2011) 1375–1382.
[8] M.M. Rad, H. Fathallah, L.A. Rusch, Fiber fault PON monitoring using optical coding: effects of customer geographic distribution, IEEE Trans. Commun. 58 (4) (2010).
[9] M.M. Rad, H. Fathallah, L.A. Rusch, Performance analysis of fiber fault PON monitoring using optical coding: SNIR, SNR, and falsealarm probability, IEEE. Trans. Commun. 58 (4) (2010).
[10] H. Fathallah, M.A. Esmail, Symmetrical Encoder for Surveillance of Ring Optical Networks, IEEE Photon. Technol. Lett. 25 (17) (2013) 1719–1722.
[11] M. Zhu, J. Zhang, D.P. Wang, X. Sun, Optimal Fiber Link Fault Decision for Optical 2D Coding-Monitoring Scheme in Passive Optical Networks, IEEE/OSA J. Opt. Commun. Netw. 8 (3) (2016) 137–147.
[12] J. Zhang, M. Zhu, Y. Lin, P. Gao, X. Sun, 2016. A Novel Codeword Assignment Strategy based on MLMW-OOCs for Fiber Fault Monitoring in Large Capacity PON. In: Asia Communications and Photonics Conference, ACP, pp. AS1D.2.
[13] M. Esmail, H. Fathallah, Physical layer monitoring techniques for TDM-passive optical networks: A survey, IEEE Commun. Surveys Tuts. 15 (2) (2013) 943–958.
[14] K. Fouli, L.R. Chen, M. Maier, Time-, wavelength-, and code-domain optical reflection monitoring for next-generation access-metro networks, Elsevier Comput. Commun. 34 (8) (2011) 1011–1021.
[15] H. Schmuck, J. Hehmann, M. Straub, Th. Pfeiffer, Embedded OTDR techniques for cost-efficient fibre monitoring in optical access networks. In: Proc. European Conference on Optical Communications, ECOC, 1–2, Sep.
[16] B. De Mulder, W. Chen, J. Bauwelinck, J. Vandewege, X. Qiu, Nonintrusive fiber monitoring of TDM optical networks, IEEE J. Lightwave Technol. 25 (1) (2007) 305–317.
[17] G. Amaral, J. Dias Garcia, L. Herrera, G. Temporao, P. Urban, J. von der Weid, Automatic fault detection in WDM-PON with tunable photon counting OTDR, IEEE J. Lightwave Technol. 33 (24) (2015) 5025–5031.
[18] G.P. Temporao, G.V. Faria, P.J. Urban, J. p. Weid, 2013. Fault location in passive optical networks using T-OTDR and wavelength-selective isolators. In: Optical Fiber Communication Conf. and the Nat. Fiber Optic Engineers Conf.(OFC/NFOEC), paper NM2L4.
[19] D. Iida, N. Honda, H. Izumita, F. Ito, Design of identification fibers with individually assigned brillouin frequency shifts for monitoring passive optical networks, IEEE J. Lightwave Technol. 25 (5) (2007) 1290–1297.
[20] N. Honda, D. Iida, H. Izumita, Y. Azuma, In-service line monitoring system in PONs using 1650 nm Brillouin OTDR and fibers with individually assigned BFSs, IEEE J. Lightwave Technol. 27 (20) (2009) 4575–4582.
[21] M.P. Fernández, P.A. Costanzo Caso, L.A. Bulus Rossini, False Detections in an Optical Coding-Based PON Monitoring Scheme, IEEE Photon. Technol. Let. 29 (10) (2017) 802805.
[22] S. Zhang, W. Ji, X. Li, K. Huang, R. Yin, Precise Failure Location and Protection Mechanism in Long-reach Passive Optical Network, IEEE J. Lightwave Technol. 34 (22) (2016) 5175–5182.
[23] W.C. Kwong, G. Yang, Optical Coding Theory with Prime, CRC Press, ISBN: 978-1-4665-6780-1, 2013.
[24] H.-C. Chen, M.-K. Chang, G.-C. Yang, W.C. Kwong, Design of a hybrid multirate asynchronous O-CDMA system: performance spectral efficiency and throughput analyses, IEEE/OSA J. Opt. Commun. Networking 7 (2015) 1034.
[25] H. Cai, H. Liang, X. Tang, Constructions of Optimal 2-D Optical Orthogonal Codes via Generalized Cyclotomic Classes, IEEE Trans. Inform. Theory 61 (1) (2015) 688–695.
[26] W.C. Kwong, G.-C. Yang, V. Baby, C.-S. Bres, P.R. Prucnal, Multiple-wavelength optical orthogonal codes under prime-sequence permutations for optical CDMA, IEEE Trans. Commun. 53 (1) (2005) 117–123.
[27] W.C. Kwong, G.-C. Yang, Multiple-length, multiple wavelength optical orthogonal codes for optical CDMA systems supporting multirate multimedia services, IEEE J. Sel. Areas Commun. 22 (9) (2004) 1640–1647.
[28] X.L. Zhou, Y. Hu, Multilength two-dimensional codes for optical CDMA systems, Optoelectron. Lett. 1 (3) (2005) 232–234.